J. Biochem. 2012;151(6):593–598 doi:10.1093/jb/mvs038

JB THE JOURNAL OF BIOCHEMISTRY

Alzheimer's disease-related protein hGas7b interferes with kinesin motility

Received January 18, 2012; accepted February 2, 2012; published online April 11, 2012

Masafumi Hidaka[1,*], Tomoe Koga[1,*], Aina Gotoh[1], Mariko Sanada[1], Keiko Hirose[2] and Takafumi Uchida[1,†]

[1]Molecular Enzymology, Department of Molecular Cell Science, Graduate School of Agricultural Science, Tohoku University, Tsutsumidori, Amamiya, Aoba, Sendai 981-8555; and [2]Research Institute for Cell Engineering, National Institute of Advanced Industrial Science and Technology, 1-1-1 Higashi, Tsukuba 305-8561, Japan

[†]Takafumi Uchida, 1-1 Amamiya, Tsutsumidori, Aoba, Sendai, Miyagi 981-8555, Japan. Tel: +81 22 717 8775, Fax: +81 22 717 8778, email: uchidat@biochem.tohoku.ac.jp

*These authors contributed equally to this work.

In the previous study, we reported the important properties of hGas7b (i) that binds to phospho-tau and facilitates microtubule polymerization and (ii) the level of hGas7b is very low in the brains of patients with Alzheimer's disease. These results led us to study the function of hGas7b in detail. We focused on the effect of hGas7b on microtubule dynamics in the absence of tau, on the assumption of healthy tau decrease in the brains of Alzheimer's disease. hGas7b binds to microtubule directly without tau, although this binding does not enhance microtubule polymerization. Excess hGas7b interferes with kinesin motility on microtubules. These results suggest that regulation to maintain an appropriate concentration of hGas7b is required for healthy neurotransmission.

Keywords: cryo-EM/hGas7b/kinesin/motility/microtubule.

Abbreviations: CBB, Coomassie brilliant blue; Cryo-EM, Cryo-electron microscopy; EGFP, enhanced green fluorescent protein; hGas7b, human growth arrest specific 7b; MAP, microtubule-associated protein.

Microtubules are polar, hollow and cylindrical polymers of α-/β-tubulin dimmers that play important roles in cellular processes such as cell division, cell motility, intracellular trafficking and cell shape maintenance (*1*). Microtubules exhibit distinct assembly–disassembly dynamics called dynamic instability, and these dynamics are essential and indispensable properties of microtubules to change the structure of cells. The intracellular dynamic behaviour of microtubules is regulated by a balance between activities of microtubule-stabilizing and destabilizing proteins (*2*) such as the family of microtubule-associated proteins (MAPs) and tau. Proteomic profiles of tumour MAPs and an understanding of the molecular mechanisms of their expression will enable us to design more effective strategies for use of microtubule-targeting agents in cancer chemotherapy (*3*).

Human growth arrest-specific 7b (hGas7b) is predominantly expressed in brain tissues, including the cerebral cortex, hippocampus and cerebellum (*4*). hGas7b has been found to interact with cytoskeletons, including actin filaments and microtubules (*5*, *6*), and involved in controlling growth arrest and inducing apoptosis of neuroblastoma cells in response to various stimuli (*7*). We have found that (i) hGas7b binds to phosphorylated tau, and shows a synergistic effect with tau on promotion of microtubule polymerization and (ii) the levels of hGas7b protein dramatically decreased in the brains of patients with Alzheimer's disease (*8*). To further understand how hGas7b affects on the microtubule dynamics, we have studied properties of hGas7b at molecular level, and revealed that hGas7b enhances microtubule polymerization in the presence of tau by stabilizing sheet intermediates and suppressing the rapid microtubule de-polymerization (*6*).

Our results strongly suggest that hGas7b contributes to the maintenance of neural functions by cooperating with tau; therefore, enhancement of hGas7b function could be an effective strategy for recovering from pathogenesis such as Alzheimer's disease. On the other hand, Hung and Chao (7) have reported that over-expression of Gas7 isoform enhances cisplatin-induced apoptosis in mouse neuroblastoma Neuro2A cells, and we consider a possibility that excess hGas7b causes microtubule-related pathologies besides Alzheimer's disease (*8*). Therefore, it is still required to elucidate whether the excess hGas7b shows adverse effect on the microtubule dynamics In this study, we focus on the role of hGas7b in the absence of tau to clarify the direct correlation between hGas7b and microtubule dynamics, and report that hGas7b binds to microtubules and that excess accumulation of hGas7b on microtubules blocks kinesin movement.

Materials and Methods

Reagents and antibodies

Anti-Gas7 antibody was prepared as described in a previous study (*8*). Anti-tubulin monoclonal antibody was purchased from Sigma-Aldrich (MO, USA).

Protein preparation

Tubulin proteins were prepared from bovine brain by the PIPES buffer method, as described by Castoldi and Popov (*9*). As described in our previous study,

SDS–PAGE and western blot analysis ensured the purity of the tubulin, which was not contaminated with tau (*8*). Paclitaxel-stabilized microtubules were obtained by polymerization of 200 μM tubulin in PM buffer [100 mM PIPES–KOH (pH 6.9), 2 mM $MgCl_2$, 1 mM DTT and 5 mM EGTA] containing 200 μM paclitaxel and 1 mM GTP at 37°C for 15 min. $(His)_6$-tagged proteins of hGas7b and enhanced green fluorescent protein (EGFP)-fused hGas7b (EGFP-hGas7b) were expressed and purified as previously described (*8*). Expression plasmids harbouring $(His)_6$-tagged kinesin KIF5A (560 amino acids) were kindly provided by Atsuko Iwane (*10*). *Escherichia coli* cells were grown in LB medium containing 50 mg/l of kanamycin. Protein expression was induced by adding of isopropyl 1-thio-β-D-galactoside (final, 0.4 mM). After cultivation for 5 h at 23°C, the cells were collected by centrifugation and then suspended in lysis buffer [50 mM PEPS (pH 7.8), 300 mM potassium acetate, 1 mM $MgCl_2$, 0.1 mM EGTA, 1 mM ATP, 5 mM β-mercaptoethanol, 10 μg/ml leupeptin, 1 mM PMSF and 0.2 mg/ml lysozyme]. The suspension was sonicated and then centrifuged. The supernatant was subjected to Ni–NTA column (Qiagen, Hilden, Germany) and purified, according to the manufacturer's instructions. The concentrations of all proteins were determined by BCA protein assay kit (Pierce, Illinois, USA) standardized using bovine serum albumin. Proteins were analysed by using western blot analysis, according to our previously published protocol (*11*).

Co-sedimentation and pull-down assay

To determine the direct interaction between microtubule and hGas7b, 50 μM of paclitaxel-polymerized microtubule solution was mixed with hGas7b (2 μM). The mixtures (25 μl) were incubated on ice for 10 min and then centrifuged at 100,000 *g* at 4°C for 20 min. The precipitates were re-suspended in 25 μl PM buffer, and the supernatants and precipitates were subjected to SDS–PAGE. To determine the direct interaction between kinesin and hGas7b, 1 μM of kinesin was mixed with hGas7b (His-tagged, 2 μM). The mixtures (25 μl) were incubated with 30 μl of Ni–NTA resin (Qiagen) on ice for 10 min, and resin were washed twice with 300 μl of PM buffer. Then, the mixtures were centrifuged at 10,000 *g* at 4°C for 5 min, and precipitated resins were subjected to SDS–PAGE. To investigate the effect of hGas7b on microtubule–kinesin interactions, the paclitaxel-polymerized microtubule solution was mixed with kinesin (0.35 μM) and various concentrations (final, 0–6 μM) of the hGas7b. The mixtures (25 μl) were incubated at 37°C for 20 min and then centrifuged at 24,000 *g* at 30°C for 20 min. The precipitates were re-suspended in 25 μl PM buffer, and the supernatants and precipitates were subjected to SDS–PAGE. Gels were stained with Coomassie brilliant blue (CBB), and quantification of soluble/precipitated hGas7b and kinesin was performed by using Multi Gauge (Fuji Film, Japan).

Analysis of binding of hGas7b on microtubules

In vitro binding assays were conducted in flow chambers (chamber volume, 15 μl). Paclitaxel-stabilized microtubules (40 μM) were introduced in a flow chamber coated with 100 nM anti-α-tubulin antibody and blocked with bovine serum albumin. EGFP or EGFP-hGas7b proteins (0.1 μM each) were subsequently added into the chamber and observed at 25°C using both dark-field microscope and fluorescence microscopes (Olympus BX51). Microtubules polymerized in the presence of hGas7b were also examined by Cryo-EM as described previously (*6*, *12*).

Gliding assay

Gliding assays were performed according to the standard methods (*13*) with some modifications. Gliding assays were performed using rhodamine-labelled microtubules and a fluorescence microscope (BX51, Olympus, Japan). Paclitaxel-polymerized microtubules were labelled with rhodamine at 33°C for 30 min, layered over a 70% sucrose cushion and subjected to centrifugation. A kinesin solution (0.35 μM kinesin and 0.2 mg/ml casein in PM buffer) was introduced into flow chambers that consisted of a streptavidin-coated slideglass (Arrayit, CA, USA), a pair of spacers and a cover slip. After incubation for 1 min at 25°C, a casein solution (0.5 mg/ml casein and 100 mM KCl in PM buffer) was perfused, and the chambers were further incubated for 0.5 min at 25°C. Next, the microtubule solution (0.16 μM rhodamine-labelled microtubule and 10 μM paclitaxel in casein solution) was perfused. After incubation for 2 min at 25°C, an ATP solution containing the hGas7b (1 mM ATP, 20 μg/ml catalase, 20 mM glucose, 100 μg/ml glucose oxidase, 0.14 M β-mercaptoethanol and various concentrations of the hGas7b) was perfused to initiate the motor reaction. The microtubule movements were observed at 25 ± 3°C. Motility images were recorded using a CCD camera (DR-328G, Andor, UK), and analysed by NIS Element (Nikon, Japan).

Results

hGas7b binds to microtubule independently of tau

In this report, we further examined the direct effect of hGas7b on microtubules by using 'pure tubulin' prepared by PIPES buffer method (*9*). The absence of tau in the pure tubulin solution was confirmed by the western blot analysis, as previously described (*8*).

The results of a co-sedimentation assay showed that hGas7b (2 μM) precipitates with microtubules (50 μM) (Fig. 1A), suggesting that hGas7b binds to microtubules in the absence of tau. To further validate the association of recombinant EGFP-hGas7b with the microtubules, we used a dark-field microscope (Fig. 1B). Fluorescence derived from EGFP was overlayed on the microtubule, confirm the binding of hGas7b to microtubule.

Microscopy of paclitaxel-polymerized microtubule incubated with hGas7b

The rhodamine-labelled microtubules were incubated with various concentrations of EGFP-hGas7b and

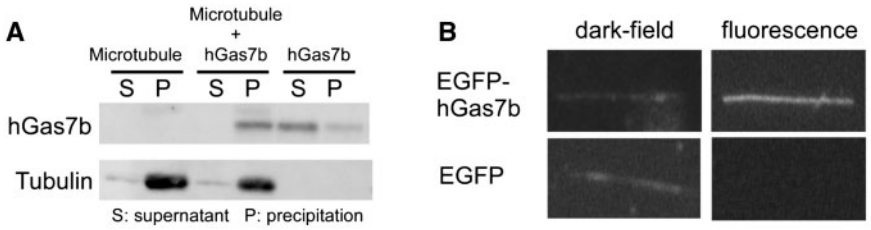

Fig. 1 Direct binding of hGas7b to microtubule. Microtubules were polymerized with pure tubulin and stabilized with paclitaxel. (A) hGas7b was incubated with microtubule solution on ice and centrifuged at 100,000 *g*. The supernatant and precipitate were analysed using western blot analysis with anti-Gas7 and tubulin, respectively. (B) Binding of EGFP-hGas7b to microtubule; the mixture of recombinant EGFP-hGas7b (0.1 μM) prepared from bovine brains was added to the paclitaxel-stabilized microtubules, and analysed with a fluorescence and dark-field microscopes.

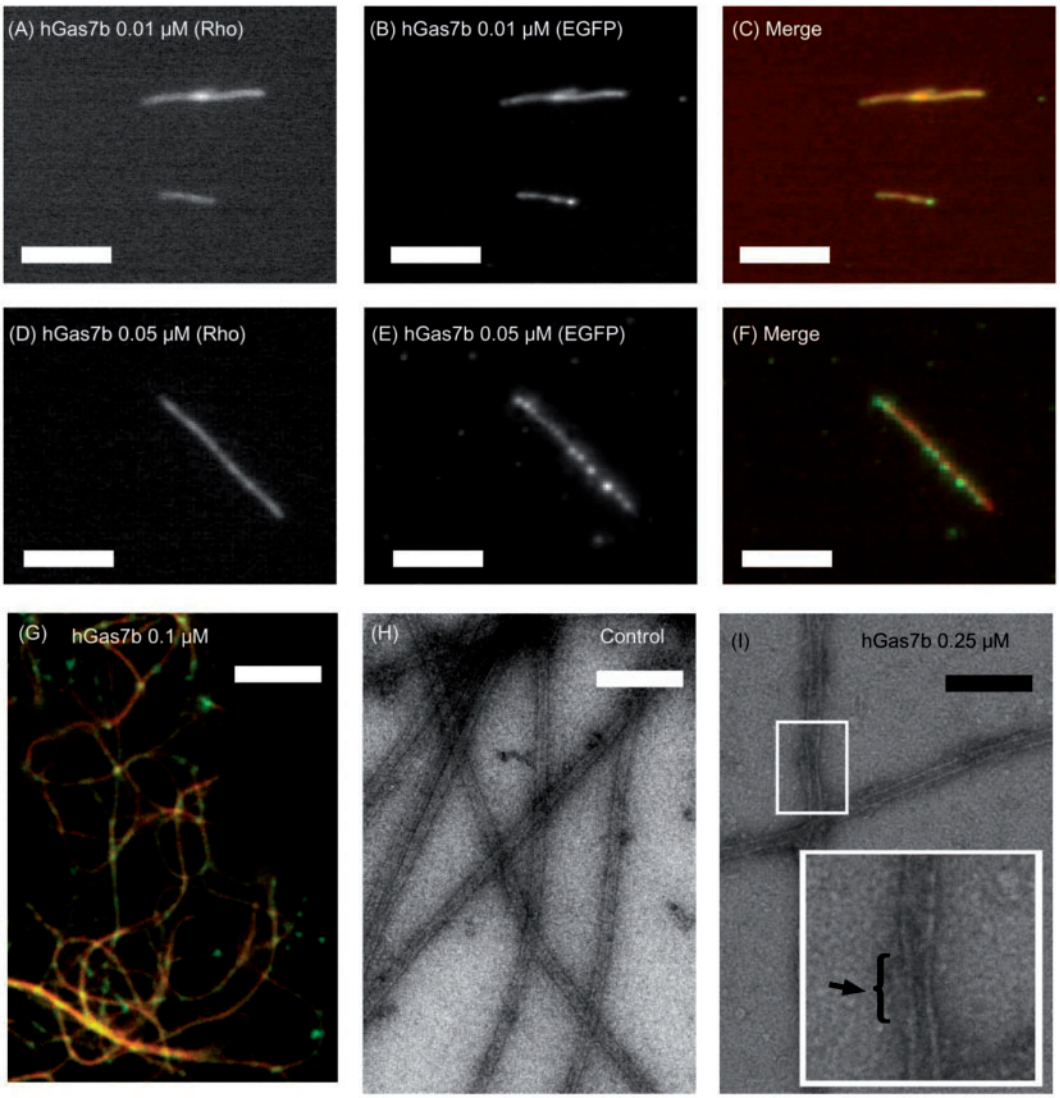

Fig. 2 Microscopy images of rhodamine-labelled microtubules (A–G). Rhodamine-labelled microtubules were incubated with 0.01 μM (A–C) and 0.05 μM (D–F) of hGas7b. (G) Image of tangles of rhodamine-labelled microtubules incubated with and 0.1 μM hGas7b. Fluorescence derived from rhodamine (A, D) and EGFP (B and E) was recorded using a CCD camera (DR-328G, Andor, UK). Scale bars: 10 μM (A–C and G) and 20 μM (D–F). Cryo-EM images of paclitaxel-polymerized microtubule without hGas7b (H) and incubated with 0.25 μM of hGas7b (I). Scale bars, 200 nm. The parts of narrowed microtubule were indicated by arrows.

subjected to microscopic analyses (Fig. 2). The fluorescence intensity derived from EGFP was uniformly distributed over the microtubule surface at low EGFP-hGas7b concentrations (0.01 μM; Fig. 2A–C). On the other hand, localization of EGFP fluorescence signals were detected at higher EGFP-hGas7b concentrations (0.05 μM, Fig. 2D–F), and excess EGFP-hGas7b (0.1 μM) resulted in tangle formation (Fig. 2G). Next, we used Cryo-electron microscopy (Cryo-EM) to analyse the microtubule structure at

high resolutions (Fig. 2H and I). In the absence of hGas7b, the structures of paclitaxel-polymerized microtubules exhibited uniform width (Fig. 2H). Conversely, the width of paclitaxel-polymerized microtubules incubated with hGas7b (0.25 μM) were partially narrowed (Fig. 2I, indicated by arrow) on the Cryo-EM image.

Gliding assay

We measured the movements of rhodamine-labelled microtubules under various concentrations of EGFP-hGas7b (Fig. 3). When the ATP solution containing 0.1 μM EGFP was perfused, >80% of microtubules glided smoothly (Fig. 3E). On the other hand, the addition of hGas7b reduced the number of moving microtubules in a concentration-dependent manner. The moving population of microtubules was analysed by measuring the distance moved from their original position after 15 s (Fig. 3F). The mean distance in the EGFP was 3.76 μM; the microtubules moved at a velocity of 0.25 μM/s. When hGas7b was present, the run distance of the microtubules decreased in a concentration-dependent manner (Fig. 3F).

Co-precipitation of microtubule/kinesin in the presence of hGas7b

A co-sedimentation assay was performed to determine whether the hGas7b interfered with the binding of kinesin to microtubules. Amount of bound and unbound kinesin to microtubule were quantified by SDS–PAGE analysis as shown in Fig. 4A. Soluble kinesin was slightly increased on addition of hGas7b.

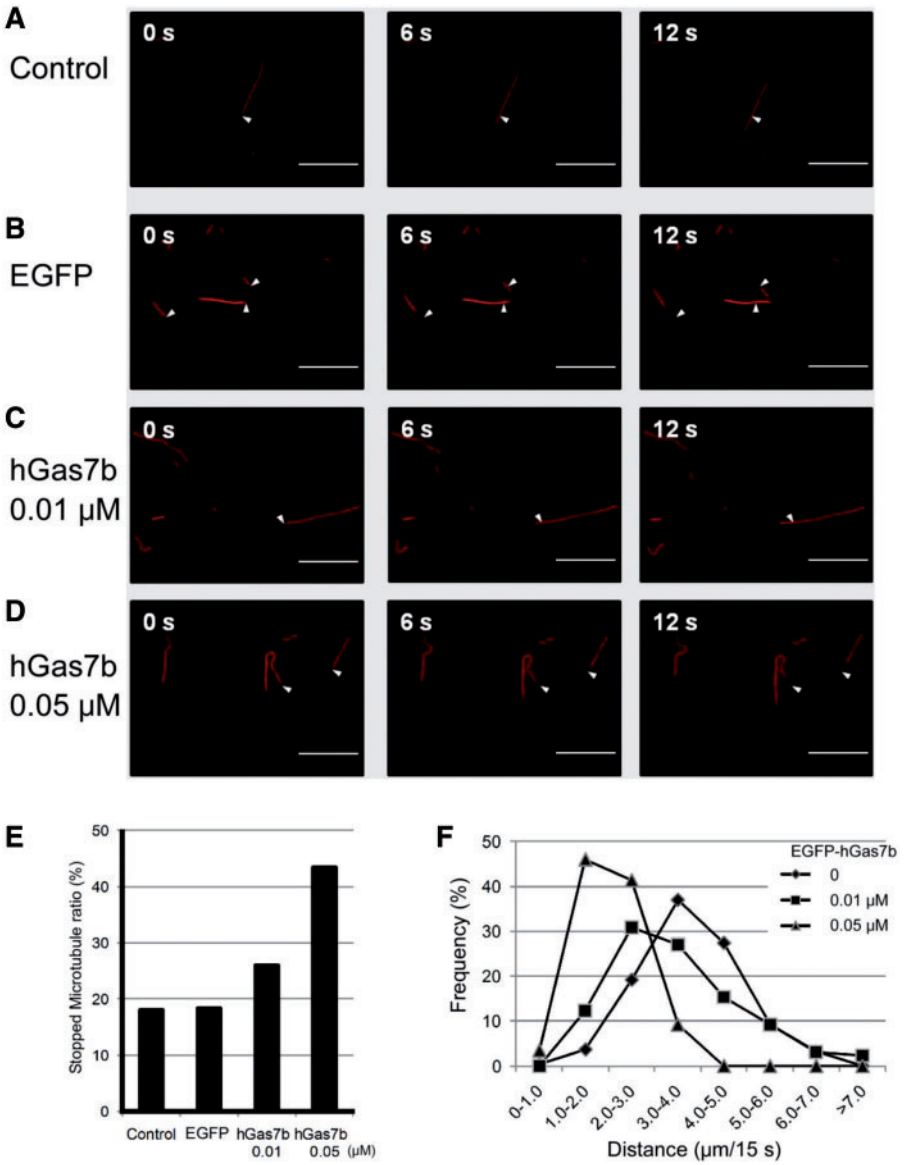

Fig. 3 Time course of the movements of microtubules in *in vitro* gliding assay. The movements of the microtubules in the (A) absence or (B) presence of 0.1 μM EGFP, (C) in the presence of 0.01 μM EGFP-hGas7b and (D) in the presence of 0.05 μM EGFP-hGas7b. Scale bars: 10 μM. (E) The frequency of the arrested microtubules in the presence of the hGas7b. (F) The distributions of the distances that microtubule moved in the presence of EGFP-hGas7b. Various concentrations (0, 0.01 and 0.05 μM) of EGFP-hGas7b were added to the gliding buffer. The total number of microtubules measured was >140 for each concentration of EGFP-hGas7b.

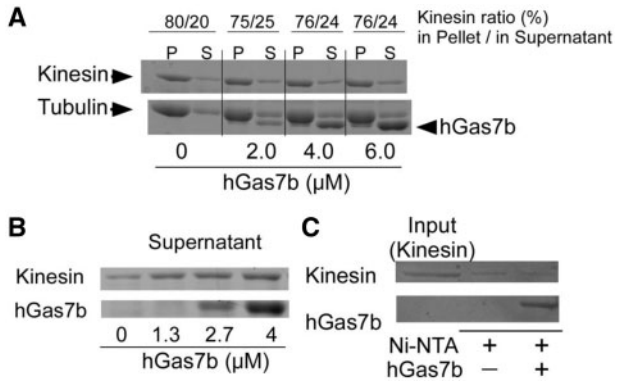

Fig. 4 Competition of hGas7b and kinesin for binding to microtubules. (A and B) Various concentrations of hGas7b and a constant concentration of kinesin (0.35 μM) were mixed with the paclitaxel-stabilized microtubules. The mixtures were incubated, centrifuged and then subjected to SDS–PAGE analysis and stained by CBB. P, Pellet; S, Supernatant. Amount of knesin ratio in pellet/supernatant were estimated by Multi Gauge. The amounts of soluble fraction subjected to SDS–PAGE were (A) 5 μl and (B) 15 μl. (C) The pull-down assay using kinesin and Ni–NTA carrying recombinant His-tagged hGas7b. Kinesin (1 μM) was mixed with hGas7b (2 μM). Captured proteins were analysed by SDS–PAGE and stained by CBB.

The amount of soluble fraction subjected to SDS–PAGE in Fig. 4B was increased as to clarify the increment of soluble kinesin. Next, a pull-down assay was performed to determine whether the hGas7b directly bound to kinesin. As shown in Fig. 4C, the amount of kinesin bound to Ni–NTA resin were not affected by addition of hGas7b.

Discussion

Function of hGas7b on microtubule dynamic instability

The process of microtubule elongation is thought to consist of two stages: formation of a tubulin sheet structure and its closure of the sheet into a tube (*14*, *15*). Closure of sheets does not require GTP hydrolysis (*16*), suggesting that GTP hydrolysis occurs concurrently with or after the sheet folds into a cylindrical structure. Our previous results demonstrate that hGas7b stabilizes the sheet structure of the microtubules together with tau, and this stabilization results from the suppression of the microtubule catastrophe (*6*). In this report, our results showed that hGas7b binds to microtubules directly (Fig. 1A). As seen in Fig. 2A–C, hGas7b uniformly covers the whole surface of the microtubule. Interestingly, we observed regions of strong fluorescence intensity of EGFP-hGas7b with increasing concentrations of hGas7b (Figs 2D–F). Furthermore, when the polymerized microtubules were incubated with high concentration of hGas7b (0.1 μM), microtubule and hGas7b formed tangles (Fig. 2G), indicating that excess hGas7b adheres to the microtubule and might results in cross-linking of the microtubules. The detailed correlation between microtubule morphology and deposition of hGas7b was further analysed by using Cryo-EM (Fig. 2H), and the Cryo-EM images revealed that the deposition of hGas7b partially narrowed the microtubule width. These results indicate that high concentrations of hGas7b deform the polymerized microtubule morphology.

hGas7b interfere kinesin motility

The addition of hGas7b reduced the population of moving microtubules (Fig. 3E) and/or stalled velocities of rhodamine-labelled microtubules (Fig. 3F) in a concentration dependent manner, indicating that adhesions of hGas7b to the microtubule surface interrupted kinesin movement. One possible explanation for this is that hGas7b competes with the kinesin for the binding site on the microtubule surface, and therefore, high concentrations of hGas7b directly interrupt kinesin binding and motility. It is also possible that hGas7b adheres to the microtubule surface in regions different from the kinesin binding site and consequently deforms to the microtubule structure, thus preventing the binding of kinesin. We attempted to clarify the mechanism by a sedimentation and a pull-down assay. Although decrease of bound kinesin were obscure under our conditions, increase of soluble kinesin was observed on addition of hGas7b, indicating that hGas7b interfered kinesin–microtubule interaction (Fig. 4A and B). On the other hand, hGas7b did not form direct interaction with kinesin (Fig. 4C). It should be noted that accuracy of the analysis could be questioned because quantification of kinesin and hGas7b were based on SDS–PAGE analysis. Statistical analysis may have to be performed by using RI-labelled protein. However, we have attempted multiple co-sedimentation assay ($n > 3$), and tendency of increase of unbound kinesin to microtubule corresponding increase in hGas7b concentration was observed. Therefore, we concluded that excess hGas7b affects the microtubule morphology and inhibits the motility of kinesin motor proteins that are involved in cell division and intracellular transport by interfering with the interaction between kinesin and the microtubule.

Correlation between physiological functions of hGas7b and biological implications

Tau proteins are abundant in neurons of the central nervous system, and defective tau proteins can result in dementias such as Alzheimer's disease. Our previous results indicated that hGas7b enhances the polymerization function of tau even at low concentrations (10 nM) (*8*).

In this study, *in vitro* analysis showed that hGas7b binds directly to the microtubule and participates in the microtubule dynamics in the absence of any other MAPs. Conversely, high concentrations of hGas7b deform the microtubules, thereby interfering with the interaction between the microtubule and kinesin. These results suggested that an adequate concentration of hGas7b might be required for microtubule maintenance, but its excess can cause interruption of cell motility or intracellular trafficking.

Acknowledgements

The authors thank Ayako Fujita and Wataru Sakamoto for technical help, Atsuko Iwane for the gift of kinesin expression vector, and Hideo Higuchi and Taketoshi Kambara for helpful discussion.

Funding

The Nakajima Foundation; The Ministry of Education, Culture, Sports, Science and Technology of Japan, Grant-in-Aid for Scientific Research [20228006 to T. U.].

Conflict of interest

None declared.

References

1. Alberts, B., Johnson, A., Lewis, J., Raff, M., Roberts, K., and Walter, P. (2002). *Molecular Biology of the Cell*, 4th edn. Garland Science, New York.
2. Andersen, S.S. (2000) Spindle assembly and the art of regulating microtubule dynamics by MAPs and stathmin/Op18. *Trends Cell Biol.* **10**, 261–267
3. Bhat, K.M.R. and Setaluri, V. (2007) Microtubule-associated proteins as targets in cancer chemotherapy. *Clin. Cancer Res.* **13**, 2849–2854
4. Ju, Y.T., Chang, a.C., She, B.R., Tsaur, M.L., Hwang, H.M., Chao, C.C., Cohen, S.N., and Lin-Chao, S. (1998) Gas7: a gene expressed preferentially in growth-arrested fibroblasts and terminally differentiated purkinje neurons affects neurite formation. *Proc. Natl. Acad. Sci. USA* **95**, 11423–11428
5. She, B.-R., Liou, G.-G., and Lin-Chao, S. (2002) Association of the growth-arrest-specific protein Gas7 with F-actin induces reorganization of microfilaments and promotes membrane outgrowth. *Exp. Cell Res.* **273**, 34–44
6. Uchida, T., Akiyama, H., Sakamoto, W., Koga, T., Yan, K., Uchida, C., Hirose, K., and Itoh, T.J. (2009) Direct optical microscopic observation of the microtubule polymerization intermediate sheet structure in the presence of Gas7. *J. Mol. Biol.* **391**, 849–857
7. Hung, F.-C. and Chao, C.C.-K. (2010) Knockdown of growth-arrest-specific gene 7b (gas7b) using short-hairpin RNA desensitizes neuroblastoma cells to cisplatin: implications for preventing apoptosis of neurons. *J. Neurosci. Res.* **88**, 3578–3587
8. Akiyama, H., Gotoh, A., Shin, R.-W., Koga, T., Ohashi, T., Sakamoto, W., Harada, A., Arai, H., Sawa, A., Uchida, C., and Uchida, T. (2009) A novel role for hGas7b in microtubular maintenance: possible implication in Tau-associated pathology in Alzheimer disease. *J. Biol. Chem.* **284**, 32695–32699
9. Castoldi, M. and Popov, A.V. (2003) Purification of brain tubulin through two cycles of polymerization-depolymerization in a high-molarity buffer. *Protein Expres. Purif.* **32**, 83–88
10. Watanabe, T.M., Yanagida, T., and Iwane, A.H. Single molecular observation of self-regulated kinesin motility. *Biochemistry* **49**, 4654–4661
11. Akiyama, H., Shin, R.-W., Uchida, C., Kitamoto, T., and Uchida, T. (2005) Pin1 promotes production of Alzheimer's amyloid beta from beta-cleaved amyloid precursor protein. *Biochem. Biophy. Res. Commun.* **336**, 521–529
12. Hirose, K. and Amos, L.A. (2007) High-resolution structural analysis of the kinesin-microtubule complex by electron cryo-microscopy. *Methods Mol. Biol.* **392**, 213–230
13. Vale, R.D., Reese, T.S., and Sheetz, M.P. (1985) Identification of a novel force-generating protein, kinesin, involved in microtubule-based motility. *Cell* **42**, 39–50
14. Chretien, D., Fuller, S.D., and Karsenti, E. (1995) Structure of growing microtubule ends - 2-dimensional sheets close into tubes at variable rates. *J. Cell Biol.* **129**, 1311–1328
15. Kirschner, M.W., Honig, L.S., and Williams, R.C. (1975) Quantitative electron-microscopy of microtubule assembly *in vitro*. *J. Mol. Biol.* **99**, 263–276
16. Wang, H.W. and Nogales, E. (2005) Nucleotide-dependent bending flexibility of tubulin regulates microtubule assembly. *Nature* **435**, 911–915